Status of the TNO Model Chain Groningen 2023

TNO Public ⟩ TNO 2023 R11795
11 October 2023

Energy & Materials Transition
www.tno.nl
+31 88 866 42 56
info@tno.nl

TNO 2023 R11795 – 11 October 2023

Status of the TNO Model Chain Groningen 2023

Author(s)	M.P.D. Pluymaekers, D.A. Kraaijpoel, F.M. Aben, S. Osinga
Classification report	TNO Public
Title	TNO Public
Report text	TNO Public
Number of pages	29 (excl. front and back cover)
Number of appendices	0
Sponsor	Ministry of Economic Affairs and Climate Policy
Project name	pSDRA 2023
Project number	060.56081

Summary

This report decribes the results of ongoing model development in relation to the public Seismic Hazard and Risk Analysis (pSHRA) Groningen and the technical status of the TNO Model Chain Groningen as of October 1, 2023. It also provides an overview of the TNO-recommended model components in the event that the pSDRA 2024 has to be executed for the “Vaststellingsbesluit 2024/2025”.

Activity rate model developments
With the immediate cessation of the Groningen gas production per October 1, 2023, the focus of model development has been on describing the current post-production seismic behavior in the Seismological Source Model (SSM). This has been encouraged by the observation that in the most recent gas years the mismatch between predicted and observed event counts can unlikely be justified as variations within the model confidence bandwidth. Underprediction of the mean event rate can be caused by not taking physical delay mechanisms into account in the model. Underprediction of the variation of the event rate can be caused by a change in the intensity of clustering of events and aftershock rates.

Delays in reservoir compaction behavour have been accounted for by the development and implementation of a Rate Type isotach Compaction Model (RTiCM) in the SMM. We have modified the SSM by including inelastic time-dependent reservoir compaction in addition to the linear elastic compaction. Although, the modified RTiCM-based SSM solves the mismatch between observed and predicted field-wide temporal event counts, we suggest incorporating both the linear elastic and the RTiCM-based SSM into the TNO Model Chain logic tree. The leave-one-out cross-validation (LOO-CV) technique yields approximately equal weights in the logic tree, i.e., 50% linear elastic and 50% RTiCM.

Delays in seismicity have been assessed by the implementation of a Rate-and-state friction based component in the SSM. The TNO-implementation reveals that the Rate-and-state model, both in the classical Dieterich (1994) formulation, and after inclusion of a threshold stress parameter below which the system remains seismically inactive (Heimisson, 2022), does not provide a viable alternative to the extreme threshold failure model by Bourne et al. (2017) and its variations. Therefore, a Rate-and-state friction based componenent is not a suitable candidate for adoption in the SSM of the TNO Model Chain or in the pSHRA Groningen.

b-value model weighting
We compare the performance of several magnitude models in combination with a number of functional forms in a leave-one-out cross-validation (LOO-CV) test on both the elastic and the RTiCM model. The magnitude models currently included in the logic tree of the Model Chain Groningen predict b-values conditional on stress. However, Kraaijpoel et al. (2022) showed that reservoir thickness outperforms stress as a predictor for b-values. Both the elastic model and the RTiCM model conditioned on reservoir thickness perform better than the models conditioned on stress. A combination of a step model conditioned on thickness and a linear model conditioned on stress optimizes the results. Averaging the weight distributions for the linear elastic and the RTiCM models yields a proposed weight distribution of a 70% step thickness and a 30% linear stress dependent b-value model.

SSM implementation enhancements

Several enhancements towards a more uniform and unambiguous codebase are implemented. The underlying physical-statistical principals and model assumptions do not change. Overall, the impact on the model results (seismicity rate) is very minimal.

Other relevant studies

- The most fragile buildings on 'wierden' (anthropogenic dwelling mounds) with LPR between 10^{-5} and 10^{-6} experience a 2.5 to 3 times higher risk after application of a wierden amplification factor in Ground Motion Models (GMM) V6 and V7. Validation of the penalty factor based on GMM-V6 is yet required for future usage in the pSHRA.
- The spatiotemporal prediction of pore pressure within the Groningen reservoir is an input parameter for the pSHRA. The Dynamic model is updated, recalibrated, and converted from the proprietary Shell MoReS/Dynamo software package to the widely used Eclipse software package (Schlumberger) by NAM.
- Despite improved statistical performance of the 2023-recalibrated SSM by NAM, the recalibration still underpredicts the total number of observed events significantly.

Recommended models in pSHRA 2024

In the event of executing pSHRA 2024, TNO proposes to adopt the newly introduced TNO-2023 SSM, GMM-V7 and the TNO-2020 FCM. The latter two are unchanged as proposed by TNO in 2022. TNO-2023 SSM is based on TNO-2020 SSM, with the following changes:

- Aforementioned SSM implementation enhancements.
- Aforementioned 50%-50% logic tree weighting of linear compaction and RTiCM based activity rate models.
- Aforementioned logic tree weights of 70% step thickness and 30% linear stress dependent b-value models.

Samenvatting

Dit rapport beschrijft de resultaten van de verrichte modelontwikkeling in relatie tot de publieke Seismische Dreigings- en Risicoanalyse (pSDRA) Groningen en de technische status van de TNO Modelketen Groningen per 1 oktober 2023. Het geeft tevens een overzicht van de door TNO aanbevolen modelcomponenten in het geval dat de pSDRA 2024 wordt uitgevoerd voor het Vaststellingsbesluit 2024/2025.

Modelontwikkelingen Seismiciteit
Met de actuele stopzetting van de Groningse gasproductie per 1 oktober 2023 ligt de focus van de modelontwikkeling op de beschrijving van het huidige seismische post-productiegedrag in het Seismologisch bronmodel (SSM). Dit wordt aangejaagd door de observatie dat in de meest recente gasjaren de voorspelde en waargenomen hoeveelheid bevingen sterk afwijkt. Het is onwaarschijnlijk dat dit gezien kan worden als variaties binnen de betrouwbaarheidsbandbreedte van het model. Onderschatting van het gemiddelde aantal bevingen kan worden veroorzaakt doordat in het model geen rekening wordt gehouden met fysische vertragingsmechanismen. Onderschatting van de variatie in het aantal bevingen kan worden veroorzaakt door een verandering in de intensiteit van de clustering van hoofdschokken en het aantal naschokken.

Vertragingen in het compactiegedrag van reservoirs worden verklaard door de model-ontwikkeling en -implementatie van een Rate Type isotach Compactie Model (RTiCM) in het SMM. We hebben het SSM aangepast door inelastische tijdsafhankelijke reservoircompactie op te nemen naast lineair elastische compactie. Hoewel het aangepaste RTiCM-gebaseerde SSM de afwijking tussen waargenomen en voorspelde bevingen oplost, stellen we voor om zowel het lineair elastische als het RTiCM-gebaseerde SSM op te nemen in de logic tree van de TNO Modelketen. De leave-one-out cross-validatietechniek (LOO-CV) levert ongeveer gelijke gewichten op in de logic tree, dat wil zeggen 50% lineair elastisch en 50% RTiCM.

Vertragingen in seismiciteit zijn beoordeeld door de implementatie van een Rate-and-state frictie component in het SSM. Uit de TNO-implementatie blijkt dat het Rate-and-state model, zowel in de klassieke formulering van Dieterich (1994), als met toepassing van een spanningsdrempel voor seismische activatie (Heimisson, 2022), geen realistische oplossing biedt als alternatief voor het Extreme Threshold Failure Model van Bourne et al. (2017) en zijn variaties. Daarom is een op Rate-and-State frictie gebaseerde component geen geschikte kandidaat voor toepassing in het SSM van de TNO Modelketen of in de pSDRA.

b-waarde modelweging
We vergelijken de prestaties van verschillende magnitudemodellen in combinatie met een aantal functionele vormen in een LOO-CV-test op zowel het elastisch als het RTiCM-model. De magnitudemodellen die momenteel zijn opgenomen in de logic tree van de Modelketen voorspellen b-waarden die afhankelijk zijn van spanning. Kraaijpoel et al. (2022) toonden aan dat de reservoirdikte beter presteert dan spanning als voorspeller voor b-waarden. Zowel het elastisch als het RTiCM-model, geconditioneerd op reservoirdikte, presteren beter dan de modellen geconditioneerd op spanning. De combinatie van stapfunctie geconditioneerd op dikte en een lineaire functie geconditioneerd op spanning optimaliseert de resultaten. Het middelen van de gewichtsverdelingen voor de lineair elastische en de

RTiCM-modellen levert een voorgestelde gewichtsverdeling op van 70% voor een stapfunctie voor reservoirdikte en 30% voor een lineaire functie voor spanning in het b-waardemodel.

SSM implementatieverbeteringen

Verschillende verbeteringen naar een meer uniforme en aperte code zijn geïmplementeerd. De onderliggende fysisch-statistische uitgangspunten en modelaannames veranderen niet. Over het geheel genomen is de impact op de modelresultaten (seismiciteit) zeer minimaal.

Overige relevante studies

- De meest kwetsbare gebouwen op wierden met LPR tussen 10^{-5} en 10^{-6} ervaren een 2,5 tot 3 maal hoger risico na toepassing van een wierdenversterkingsfactor in Grondbewegingsmodel (GMM) V6 en V7. Validatie van de penalty factor op basis van GMM-V6 is nog vereist voor toekomstig gebruik in de pSDRA.
- De spatiotemporele voorspelling van de poriëndruk in het Groningenreservoir is een inputparameter voor de pSDRA. Het Dynamisch model is bijgewerkt, opnieuw gekalibreerd en geconverteerd van het eigen Shell MoReS/Dynamo-softwarepakket naar het veelgebruikte Eclipse-softwarepakket (Schlumberger) door NAM.
- Ondanks verbeterde statistische prestaties van het in 2023 opnieuw gekalibreerde SSM door NAM, geeft de herkalibratie nog steeds een aanzienlijke onderschatting van het totale aantal waargenomen bevingen.

Aanbevolen modellen in de pSDRA 2024

Bij eventuele uitvoering van pSDRA 2024 stelt TNO voor om de nieuw geïntroduceerde TNO-2023 SSM, GMM-V7 en de TNO-2020 FCM te gebruiken. Deze laatste twee blijven ongewijzigd zoals voorgesteld door TNO in 2022. TNO-2023 SSM is gebaseerd op TNO-2020 SSM, met de volgende wijzigingen:
- Voornoemde SSM-implementatieverbeteringen.
- Voornoemde 50%-50% logic tree weging van lineaire compactie en op RTiCM-gebaseerde modellen voor de seismiciteit.
- Voornoemde logic tree gewichten van 70% stapfunctie geconditioneerd op reservoirdikte en 30% lineaire functie geconditioneerd spanning in het b-waardemodel.

Contents

1 Introduction

As of 2021, the public Seismic Hazard and Risk Analysis (pSHRA) of the Groningen gas field, required for state approval of the Operational Strategy for the yearly gas production, is executed in the public domain. To fulfil this task, TNO makes use of the internally developed model toolkit: the TNO Model Chain Groningen (TNO, 2019; 2020b).

1 October 2023 marked the cessation of production from the Groningen gas field. Decommissioning of the production facilities is foreseen to start after 1 October 2024, but this decision and process has yet to be enshrined in laws and legislation. Until this is formalised the field is in stand-by mode: production can technically be resumed.
Despite the measures taken to decrease and finally cease production, the seismic activity is likely to continue for the coming years to decades. Continued research and model development on the spatiotemporal development of seismicity in Groningen is useful in the post-production phase.

1.1 Model development programme

In the most recent gas years, we observed a disparity between predicted and observed event counts that is highly unlikely to be labelled as variations within the model prediction bandwidth (Figure 1.1). This raises concerns on the SSM prediction performance for the post-production phase of the Groningen field.

Considering the observed events up to the end of the present gas year (1 October 2023) the suspicion that the model is underpredicting the event rate is still relevant.
The mismatch between de observed and modelled events can be explained by either an underprediction of the mean event rate or an underprediction of the dispersion (variation) of the event rate.
Underprediction of the mean event rate can be caused by not taking physical delay mechanisms into account in the model. The current model only addresses the diffusion of the pore pressure in the reservoir, resulting in the currently predicted trailing seismicity over the coming decades. Other mechanisms such as a delay in reservoir compaction after pressure decline that is observed in lab scale experiments and inferred from surface deformation measurements, is not accounted for. The same holds for potential delays between compaction (and thus stress change) and seismicity.
Underprediction of dispersion can be caused by a change in the intensity (or distinct visibility) of clustering of events and aftershock rates.

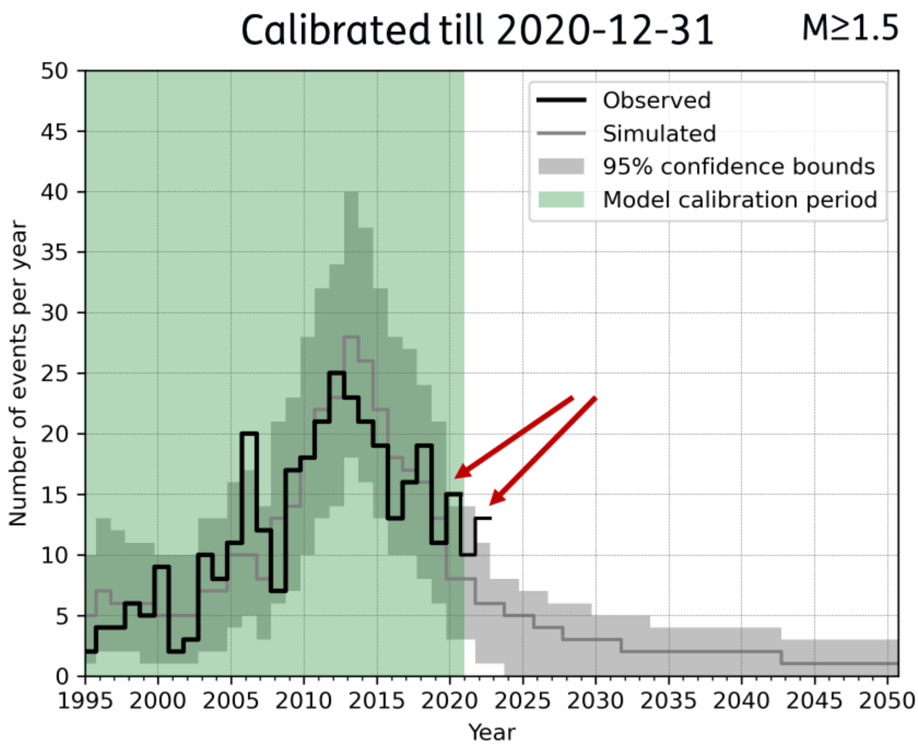

Figure 1.1: Observed vs. simulated seismic activity (events above or equal to M=1.5) summed per gas year. Horizontal axis represents time in calendar years. The model calibration period is indicated by the green area. Red arrows indicate model-observation disparities based on model calibration up to 1 January 2021.

Above-described topics were explored within the pSHRA Groningen model development programme. More distinctly, this has led to the following activities:

- Development and implementation of a Rate-type compaction based seismological source model to account for delays in reservoir compaction behaviour.
- Implementation of a Rate-and-state seismological source model to account for potential delays in seismicity.
- Exploratory analysis of clustering of events and aftershock rates. Result so far on this subject is still inconclusive and is not part of this report.

This report describes the results of ongoing model development in relation to the pSHRA with special focus on modelling the spatiotemporal development of seismicity (chapter 2) and the status of the TNO Model Chain per October 1, 2023, with proposed enhancements (chapter 3).

2 Model development

2.1 Seismicity rate models

2.1.1 Seismological Source Model with Rate Type compaction behavior

We have explored several avenues to ensure that the SSM remains capable of reliably predicting future main shock seismicity after cessation of gas production. The currently used SSM, which computes stress changes based on linear elastic reservoir compaction, cannot predict main shocks for constant or increasing reservoir pressures expected during shut-in. This may be the underlying cause for the underprediction of the observed temporal event count in recent years (TNO, 2022a).
We have modified the SSM by including inelastic time-dependent reservoir compaction in addition to the linear elastic compaction. The combination of inelastic time-dependent and instant elastic behavior results in rate dependent compaction behavior. Rate dependent compaction behavior is well known from laboratory experiments and from subsidence measurements and provides a delay mechanism in stress build-up and subsequent main shock seismicity. The compaction model that we used for this is the Rate Type isotach Compaction Model (RTiCM) (de Waal, 1986; Pruiksma et al., 2015). The RTiCM model parameters have recently been calibrated on surface subsidence data (NAM, 2021). Under some assumptions, RTiCM is straightforwardly implemented in the SSM. The modified RTiCM-based SSM solves the discrepancy between observed and predicted field-wide temporal event counts. However, no statistically better performing model was found when comparing the elastic and RTiCM-based SSM using the CSEP testing suite – hence, we suggest that both models should be incorporated into the Model Chain logic tree. To determine the relative weights, we use the leave-one-out cross-validation technique, the results of which are presented in section 2.3.

In the accompanying report “Implementation and model performance of Rate-type compaction based SSM” (TNO, 2023b), we detail:

1. The discrepancies between the elastic model and the observed seismicity.
2. The required adjustments and assumptions on the thin sheet stress model for incorporating an inelastic time-dependent compaction model such as the RTiCM.
3. A synopsis and appraisal of the Rate Type isotach Compaction Model.
4. Moving window analysis results on the performance of the elastic- and RTiCM-based SSMs.
5. CSEP consistency and comparison testing results of the elastic- and RTiCM-based SSMs.
6. In the spirit of the KEM9 sensitivity study, the impact of the RTiCM-based SSM on the risk.

2.1.2 Rate-and-State seismological model

We have investigated whether Rate and State frictional behaviour at faults (Dieterich, 1994) could provide an improved hindcast of seismicity, especially considering the underprediction of the observed event count in recent years. To do so, we implemented the Heimisson et al. (2022) formulation of the rate and state model. This paper applies a new version of the rate-and-state method to the Groningen field. Relative to Dieterich (1994) it introduces a parameter representing a 'threshold stress' below which the system remains seismically inactive. In the paper this new model appears to replicate the decline in seismicity after the onset of production limitations reasonably successfully. We have implemented this new rate-and-state formulation on the Coulomb stress changes computed with the linear elastic compaction model that is currently being used in the pSHRA. Note that Heimisson et al. (2022) use the alternative stress model by Smith et al. (2022). This alternative stress model is also fully elastic, so in terms of temporal behaviour, we do not expect the results to differ significantly.

We found that we were able to calibrate the rate-and-state seismicity model (i.e., we obtained a well-bounded posterior parameter distribution), but the calibrated model showed a poor temporal fit to the historical data (Figure 2.1). Noticeably, the seismicity responds rather slowly to changes in gas production (i.e., in changes in stress). This is due to the calibrated value of the threshold stress, which is calibrated to be very low. That is to say, the calibration virtually disables the threshold stress, reverting to the original Dieterich form, which is known to not reproduce the Groningen situation very well (see Heimisson et al., 2022 - Figure 6b).

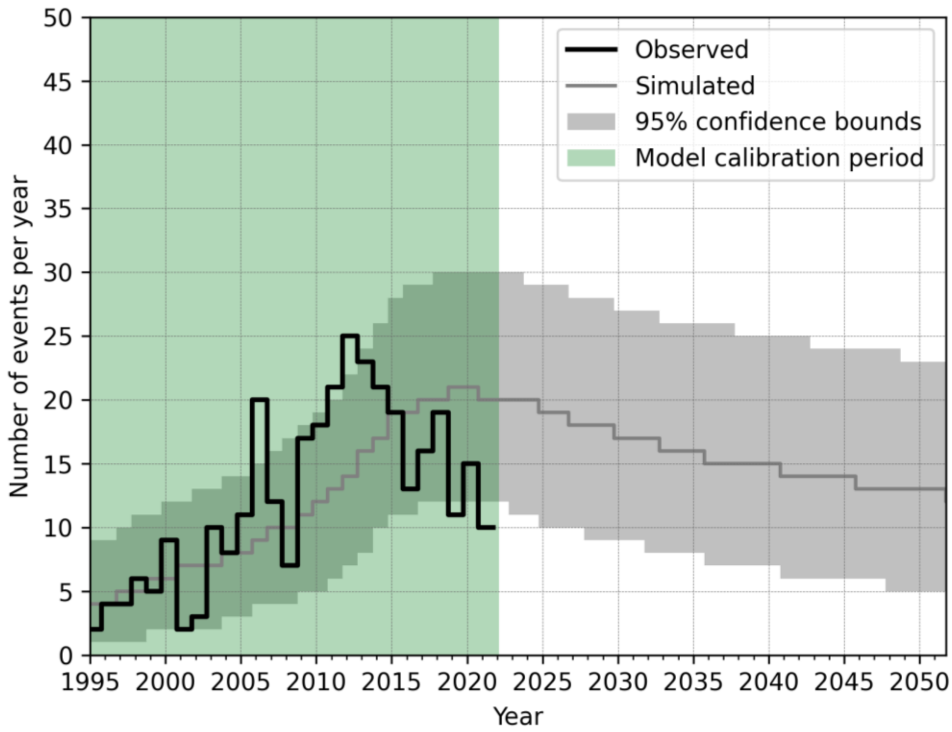

Figure 2.1: Observed vs. simulated seismic activity (events above or equal to M=1.5) per gas year. The model calibration period is indicated by the green area.

This result differs significantly from the threshold stress value obtained by Heimisson et al. (2022), who find a threshold stress value that is significantly higher, resulting in a much more direct temporal relation between stressing rate and seismicity rate (Heimisson et al., 2022 - Figure 6a).

We have identified the reason for this large discrepancy to be the difference in calibration procedure. The Heimisson et al. (2022) calibration procedure only judges the model performance in terms of temporal fit (they use a temporal likelihood function) and do not consider the spatial (or, more precisely, spatiotemporal) fit of the model. This effectively means that the threshold stress value can be calibrated to be much higher than the local stress value at events. Such a parameter choice allows the model to predicting zero event rates at the times and locations of the events present in the seismic catalogue. This is allowed under the Heimisson et al. (2022) calibration procedure, as long as the model predicts enough events elsewhere in the field to match the total number of observed events. In the TNO implementation, however, this is not allowed, as it uses a full spatiotemporal likelihood function. Note that Heimisson et al. (2022) do show a spatial event density prediction in their Figure 4. However, this figure represents an integral over time and therefore ignores the (spatio)temporal variations.

The Heimisson et al. (2022) rate-and-state implementation appears to be logically and physically inconsistent. The TNO implementation reveals that the rate-and-state model, both in the classical Dieterich (1994) formulation, and after inclusion of a threshold parameter (Heimisson, 2022), does not provide a viable alternative to the extreme threshold failure model by Bourne et al. (2017) and its variations, and is therefore not a suitable candidate for adoption in the TNO Model Chain Groningen or in the pSHRA,

2.2 SMM implementation updates

This section contains several implementation enhancements towards a more uniform and unambiguous codebase. The underlying physical-statistical principals and model assumptions do not change. Overall, the impact on the model results (seismicity rate) is very minimal, in the order of one tenth to hundredth fractional event.

2.2.1 Spatial decay ETAS-clustering in forecast

The Seismological Source Model (SSM) used in the pSHRA contains an Epidemic Type Aftershock Sequence (ETAS) clustering component on top of the Extreme Threshold Thin Sheet main shock model. The full ETAS model has a total of 6 parameters; 2 parameters (K, a) control the total aftershock productivity, 2 parameters (c, p) control the temporal decay, and 2 parameters (d, q) control the spatial decay. For the pSHRA, only K and a are calibrated, while the values for c, p, d, q are fixed.
In the current implementation (TNO, 2020a), the temporal and spatial decay is not applied in the forecast (i.e., aftershocks occur at the time and location of the mainshock).
Now that production has slowed down significantly, and is planned to cease in the immediate future, this choice has been reconsidered. There are now spatial regions of the field where the modelled main shock rate is zero, because of locally increasing gas pressures. However, the calibrated ETAS model still leads to a (very low, but) non-zero seismicity rate in these regions. The updated implementation executes the spatial decay component of ETAS in the forecast to reflect this. For now, the temporal decay has not been implemented. This effectively 'pulls forward' all aftershocks in time. We foresee a future update which also includes the temporal decay in the forecast and includes the observed, rather than the modelled, past seismicity to give a more accurate forecast of expected ETAS productivity.
The overall effect of all these updates, both in their isolated form and as a whole on the forecasted hazard and risk, is minimal.

2.2.2 Spatial contour for model calibration

The SSM is calibrated on all available Groningen earthquake data for events of M1.5 and above, recorded since 1995. The earthquake data used is provided by KNMI. This is a dataset of all induced seismic events in the KNMI network, not just in the Groningen area. To create a 'Groningen catalogue', the KNMI catalogue is filtered using the original Groningen Gas-Water contact (GWC). All events within the GWC are considered to be 'Groningen events'.
When calibrating the model in the Bayesian framework, the total modelled number of events over the calibration period is one of the inputs to the likelihood function. This total modelled number of events is an integral over time (the calibration period) and space (the modelled area of interest).
In the current implementation the spatial integral is simply taken as the sum over the entire forecast grid. It would be more appropriate to update this to consider only the forecast grid within the GWC, to keep the comparison between model and data as clean as possible. Note that for the forecast of hazard and risk, modelled seismicity outside the GWC is currently included, and this will remain in the update.
This update will lead to an increased estimate of hazard and risk, since the calibrated rate over the full grid will increase in order to match the observed rate within the GWC. We expect the effect of this update to be limited (see KEM9 study, TNO 2022c), because the vast majority of the modelled seismicity occurs within the GWC, and so the adjustment to the seismicity rate will be minimal.

2.2.3 Use KNMI unrounded database

The SSM is calibrated on all available Groningen earthquake data for events of M1.5 and above, recorded since 1995. The earthquake data used is provided by KNMI. This data is available as a direct file download (https://www.knmi.nl/kennis-en-datacentrum/dataset/aardbevingscatalogus) and through a data portal (http://rdsa.knmi.nl/dataportal/). The current implementation of the SSM uses the direct file download. In this format, the event magnitudes are rounded to one decimal place (e.g., M1.5 or M3.6). The updated implementation uses the data portal, which provides (for all intents and purposes) unrounded magnitudes. This has a very limited impact on risk (KEM9 study, TNO 2022c).

2.2.4 Temporal labelling implementation

The SSM contains several data inputs and model outputs which are labelled in time (gas pressures, earthquake observations, forecasted event rates, etc.). In the current implementation, all temporal labelling is done based on 'decimal years' (e.g., the M2.0 earthquake at 1995-04-06 08:03:43 happened at 1995.26119429). This conversion to decimal years is based on a custom implementation which accounts for leap-years. The updated implementation used the numpy.datetime64 format to express time. This cleans up the codebase and makes it more readable and maintainable. Since the numpy.datetime64 format is effectively 'second-based' rather than 'year-based' this leads to very minimal changes around leap years. For example, in the old implementation, a time difference of 1 day during 2020 (a leap year) is $1/366 \approx 0.00273224$ years, while a time difference in 2019 (a non-leap year) is $1/365 \approx 0.00273972$ years. In the updated implementation a time difference of 1 day is identical between leap years and non-leap years. Since time differences are used for temporal interpolation of gas pressures and calibration of the ETAS model, this will have some non-zero effect. However, the effect on forecasted hazard and risk is expected to be very minimal.

2.2.5 Merged calibration procedure for training and testing set

The SSM is calibrated on all available Groningen earthquake data for events of M1.5 and above, recorded since 1995. Historically, the calibration was performed on a 'training' dataset and a 'testing' dataset. This splitting of the dataset was used to assess model performance. The current implementation of the SSM still splits the dataset in two, calibrates the model on both datasets independently, and then combines the results. Although this is mathematically fully equivalent to calibrating on all the data simultaneously for the main shock model, it 'breaks' the causal chain of the ETAS model in two separate chains. The updated implementation no longer splits the dataset in two sets, but rather calibrates on the full dataset simultaneously. The expected effect on hazard and risk is very minimal.

2.3 Performance assessment and model weighting

2.3.1 Introduction

The Seismological Source Model (SSM) provides predictions or forecasts of earthquake densities and rates in space, time and magnitude. More detailed, it provides the expected number of earthquakes for a specific area, a specific timeframe, and a specific magnitude range. This can be, for example, the expected number of earthquakes for the coming gas year, for the entire Groningen field and a magnitude range of M_L=1.5 and higher. But the forecasts may also be more specific. The spatial granularity goes down to blocks of 500m x 500m, limited only by the resolution of the input data supplied by the field operator. The temporal granularity is currently fixed at entire years, either gas years or calendar years. The granularity of magnitudes is unrestricted, but magnitude counts are commonly communicated in terms of bins with a width of 1.0 magnitude unit, or in open-ended ranges (greater than, e.g., 1.5, 3.5, etc.).

It is worth emphasizing once more that the SSM does not predict the occurrence of individual earthquakes, but rather the statistics of earthquake counts in bins of finite space-time-magnitude ranges, which, in the limit of smaller and smaller bins equates to earthquake density (space/magnitude) rates (time). The modelled statistics are not directly measurable. In between the model outcomes and the observations is the earthquake excitation/recurrence process, which can be considered a random process, leading to irreducible uncertainties in event counts, also referred to as aleatoric uncertainty.

Apart from the expectation value of the event counts the SSM is also able to provide uncertainty in terms of the variance of the expected event count. The consistent treatment of uncertainties is achieved by a Bayesian approach to model parameter inference, and taking into account full posterior probability distributions for predictions.
This uncertainty may be considered of epistemic nature. The variance is partly due to the limited data available for the inference of the model parameters, but may also be related to shortcomings of the applied model that may not allow it to further reduce the variance below some limit regardless of the amount of data available. Related to the latter, epistemic uncertainty of the choice of model itself is represented on the pSHRA logic tree. Previous editions of the pSHRA have included possible alternatives for the magnitude part of the SSM, i.e., the "magnitude model" only. For the future hazard and risk analysis TNO provides alternatives for the space-time part, the "activity rate model", as well.

In the opening sentence of this section we have referred to the outcome of the SSM as being "predictions" or "forecasts" of earthquake counts. We consider predictions as the more general term, for any outcome of the model conditional on the input data. Predictions encompass also, for example, hindcasts within the space-time-magnitude domain where data was collected and used to infer the model parameters, but also outside that range, further in the past, outside the spatial domain, and/or outside the magnitude range considered. Forecasts can be considered predictions explicitly for the future.

In the seismological earthquake forecasting community it is common to make the distinction between prospective and pseudo-prospective forecasts. In principle it is possible to make forecasts for time intervals in the past, using only data from before that interval. However, although the observations from the time interval may not be used explicitly in the model parameter inference, awareness of these observations by the practitioner may inadvertently steer their model selection, their choice of input data and / or data conditioning methods. For this reason, forecasts applied to the past are referred to as "pseudo-prospective", while only true forecasts for future are considered "prospective".

Especially when forecasts are used to inform decision processes it is important to be able to assess their reliability, or in other words, to assess the predictive and forecasting performance of models. One way to do this is to evaluate the results of prospective forecasts from the past or, by lack there-off, such as when a new model is introduced, the results of pseudo-prospective forecasts. This is the approach of the Collaboratory for the Study of Earthquake Predictability (CSEP, CSEP Testing – Collaboratory for the Study of Earthquake Predictability), see also, e.g., for theoretical underpinnings, Rhoades et al. (2011), or, for software implementations, Savran et al. (2022). The CSEP tests have also been implemented by TNO and used to evaluate the performance of the seismicity rate models.

There are two main reasons, however, to also look a bit further for validation methods. First, the assessment based on (pseudo-)prospective forecasts is limited in the sense that it validates the model only on a single realization, i.e., the recent past, that used to be the future at the time of forecasting. As the (new/current) future will reveal yet other realizations, validation based on a single realization will be biased. It is therefore interesting to adopt approaches that use a larger number of validations for performance assessment. Second, the (pseudo-)prospective performance assessment does not directly provide the machinery to quantitively compare the performance of the models in such a way that it allows to assign weights (or a weighting mechanism) for combining the forecasts of several prospective models. For these two reasons we turn to leave-one-out cross-validation and model stacking in the following Section.

2.3.2 Leave-one-out cross-validation and model weighting

To make a more robust performance assessment it is essential to use a larger number of validations. However, every validation requires the separation of the available data into training and validation subsets. The maximum number of independent validation subsets that can be selected from a dataset is equal to the total number of data points. This maximum is achieved when the subsets are limited to 1 data point only. This principle is at the basis of the leave-one-out cross-validation (LOO-CV) procedure.

The LOO-CV technique has become especially attractive in the context of Bayesian model parameter inference owing to the invention of the highly efficient (approximate) evaluation technique by Vehtari et al. (2017), which requires only a single inference using the entire dataset. The leave-one-out evaluations can subsequently be approximated using Pareto-Smoothed Importance Sampling (PSIS-LOO) on the posterior distribution.

The results of LOO-CV analysis can be used directly to establish the optimal weights for a weighted sum (averaging/mixing) of probabilistic model forecasts through a procedure referred to as stacking (Yao et al., 2018). The weighting takes place on the posterior predictive distributions. The optimal weights maximize the expected log predictive density (ELPD) of the observations relative to the combined model. This is the same as the sum of the log-likelihoods values for all observations.

To make use of the PSIS-LOO technique and posterior predictive stacking we implemented a new model calibration workflow in Python PyMC ecosystem, using the PyMC package (Abril-Pla et al., 2023) for Markov Chain Monte Carlo Bayesian parameter inference, and the Arviz package (Kumar et al., 2019) for model comparison using PSIS-LOO and weight calculation. In the following sections we present the results for the activity rate model and the magnitude distribution model.

2.3.2.1 Activity rate model

We compare the performance of two seismic activity rate models. The first is the classic exponential threshold failure model by Bourne and Oates (2017) conditional on a linear elastic compaction model as implemented in slightly adapted form by TNO (2023b). The second is the same model but conditioned on the Rate-Type isotach Compaction (RTiCM) stress model as introduced in paragraph 2.1.1 and the separate reported model implementation (TNO, 2023b). We refer to the latter two references for an explanation of the differences between the two models.

The time evolution of both models, calibrated using Bayesian inference with PyMC, are displayed in **Error! Reference source not found.** and **Error! Reference source not found.**, using earthquake data (KNMI) until September 20, 2023. The mean expected event count (earthquake rate) is plotted, along with its 95% confidence bound (dark grey) representing the posterior model parameter distribution. The annual earthquake count has an additional variation around its expected value, as shown with the 95% confidence bounds in light grey. The realization, or the actual number of observed earthquakes, is provided in black.

Both the linear elastic and the RTiCM models have been subject to an LOO-CV analysis using PSIS-LOO in the Arviz implementation. The results are displayed in Figure 2.4 and Table 2.1. Figure 2.4 shows both models the ELPD, the in-sample ELPD, the LPD distributions (horizontal lines, 95% confidence range) and for the first (linear elastic) model the ELPD difference and confidence bound relative to the second (RTiCM). Here, ELPD is the main performance metric in the LOO-CV approach. ELPD stands for “expected log predictive density” and it refers to the average/mean of the pointwise LOO log-likelihood validations. The “in-sample ELPD” is the same metric when the full posterior model is used, calibrated on all events including the “left out” event. For details the reader is referred to Vehtari et al. (2017). The corresponding values are supplied in Table 2.1.

The ELPD values for both models are very similar relative to their (expected) difference. More informative than the ELPD values is the set of weights that is subsequently calculated from the PSIS-LOO results and shown in Table 2.1. The models have similar performance when evaluated over the entire history, which results in comparable weights. As shown in the model implementation documentation (TNO, 2023b), in recent years the temporal performance of the RTiCM model has been a bit better, while the spatial performance was a bit less. From the current analysis we find that overall, the differences in performance are quite balanced, leading to approximately equal weights, i.e., 50% linear elastic and 50% RTiCM.

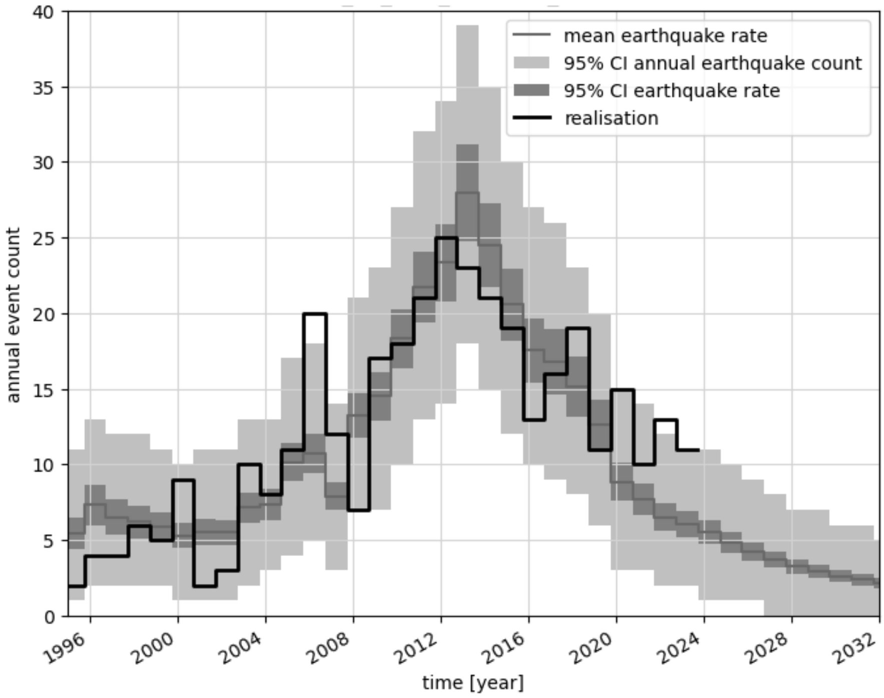

Figure 2.2: Time evolution of the annual event count distribution according to the linear elastic stress model.

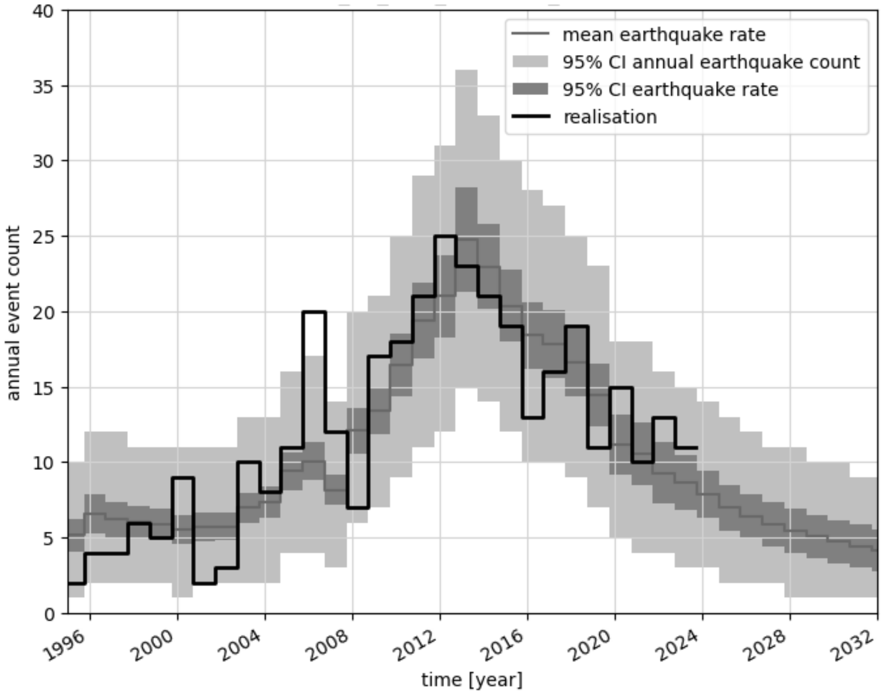

Figure 2.3: Time evolution of the annual event count distribution according to the Rate-Type isotach Compaction (RTiCM) stress model.

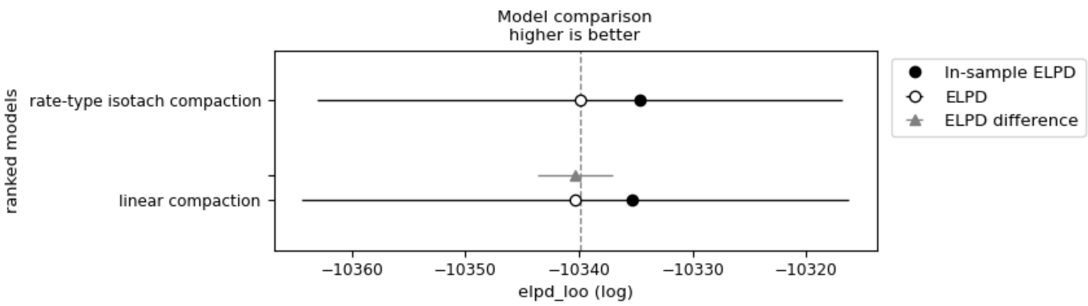

Figure 2.4: Graphical representation of the activity rate model comparison based on PSIS-LOO.

Table 2.1: PSIS-LOO statistics for the activity rate model comparison

	rank	elpd_loo	p_loo	elpd_diff	weight
Rate-Type isotach Compaction	0	-10339.91429	5.241254	0.00000	**0.510738**
linear compaction	1	-10340.35356	5.007316	0.43927	**0.489262**

2.3.2.2 Magnitude distribution model

The prediction of magnitudes in the Groningen field is performed by the magnitude distribution model. This model basically represents the Gutenberg-Richter relation, but the b-value may vary with space and time. The models currently included in the Groningen logic tree predict b-values conditional on stress. Recently, Kraaijpoel et al. (2022) have shown that reservoir thickness outperforms stress as a predictor for b-values.

To compare the performance of a number of magnitude models we submit them to a LOO-CV performance comparison test. We use both reservoir thickness and stress as a predictor in combination with a number of functional forms. Kraaijpoel et al. (2022) have shown that a step model performs well for thickness. To increase the efficiency of MCMC Bayesian inference we make a slight modification to the step model, smoothing it to a tangent hyperbolic sigmoid function with a fixed scale parameter of 5% of the (thickness/stress) range. We also include a separate “tanh” model for stress that fixes the location parameter at (incremental) stress 0, and infer the scale as a free model parameter, as this is the model currently included in the pSHRA. Also, we test linear models in both thickness and stress, as well as a constant b-value model. The test results are summarized in Figure 2.5 & Figure 2.6 and Table 2.2 & Table 2.3. We have done the experiments twice, so separate for both stress models of the previous section.

The two models conditioned on thickness perform better than the models conditioned on stress. Of the stress-conditioned models the linear variant performs better that the currently used tanh model. A subset of the posterior b-value models is displayed in Figure 2.7.

The stacking approach for determining the model weights are shown in Table 2.2 & Table 2.3 reveals that a linear combination of a step model conditioned on thickness and a linear model conditioned on stress optimizes the results. Note that the weights are not necessarily distributed according to performance. The model with a linear dependence on thickness performs better that a model with a linear dependence on stress. However, it appears that the latter has more “added value” in the linear combination. The benefits of a conditioning on thickness are already well represented by the step model. However, conditioning on stress does provide some additional predictive power, as expressed in the associated weights. The weight distributions for the linear elastic and the RTiCM models are fairly comparable. Averaging both results yields a proposed weight distribution of 70% step thickness and 30% linear stress.

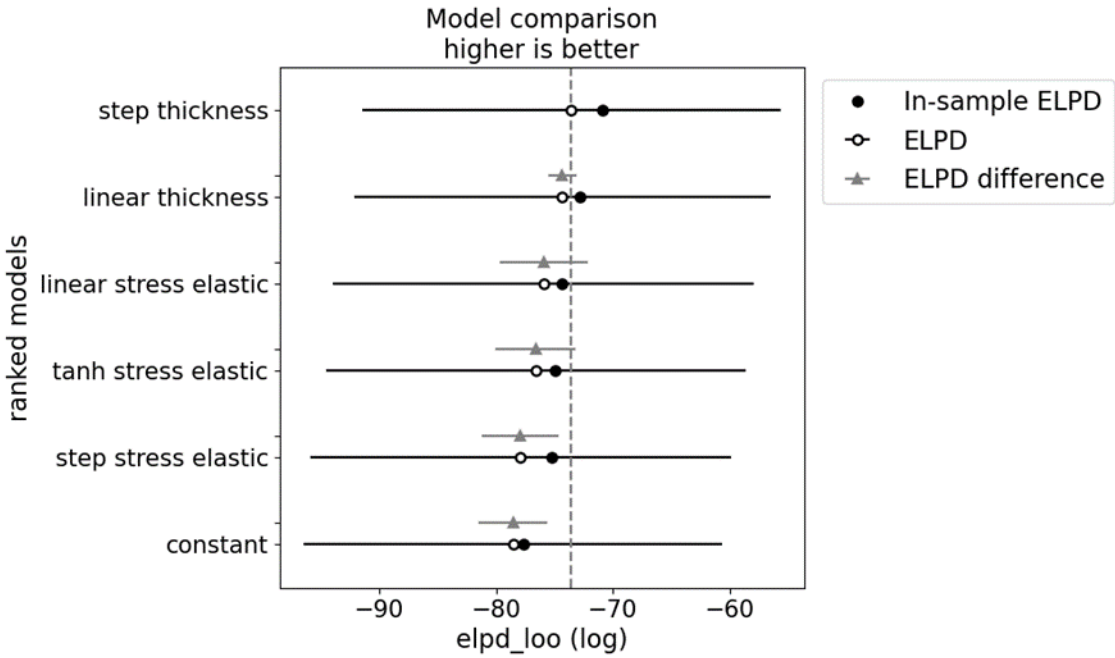

Figure 2.5: Graphical representation of the b-value model comparison based on PSIS-LOO. This figure compares a step model and a linear model conditional on reservoir thickness with three models conditional on linear elastic stress and the constant model.

Table 2.2: Results of magnitude model comparison analysis using PSIS-LOO for the linear elastic stress model.

	rank	elpd_loo	p_loo	elpd_diff	weight
step thickness	0	-73.590155	2.668605	0.000000	**6.656580e-01**
linear thickness	1	-74.337158	1.488101	0.747003	0.000000e+00
linear stress elastic	2	-75.911049	1.539483	2.320895	**3.343420e-01**
tanh stress elastic	3	-76.605201	1.657747	3.015046	0.000000e+00
step stress elastic	4	-77.894733	2.627950	4.304578	0.000000e+00
constant	5	-78.551989	0.899912	4.961834	5.129230e-14

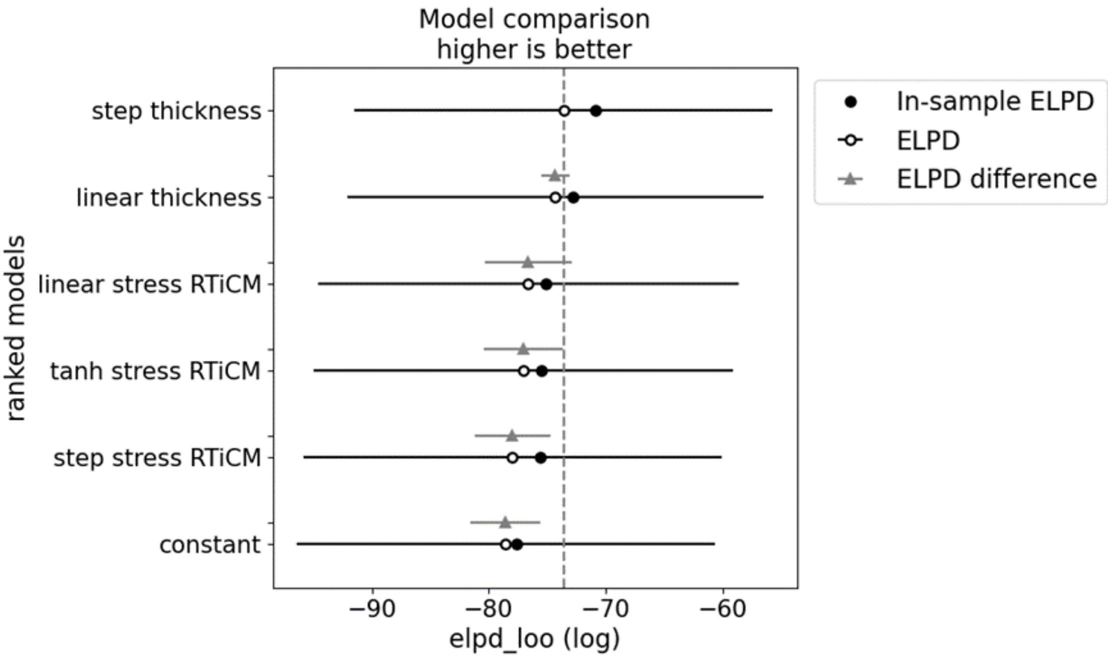

Figure 2.6: Graphical representation of the b-value model comparison based on PSIS-LOO. This figure compares a step model and a linear model conditional on reservoir thickness with three models conditional on Rate-Type isotach Compaction (RTiCM) stress, and the constant model.

Table 2.3: Results of magnitude model comparison analysis using PSIS-LOO for the Rate-Type isotach Compaction (RTiCM) stress model.

model	rank	elpd_loo	p_loo	elpd_diff	weight
step thickness	0	-73.590155	2.668605	0.000000	**7.244358e-01**
linear thickness	1	-74.337158	1.488101	0.747003	6.208497e-15
linear stress RTiCM	2	-76.621992	1.514297	3.031837	**2.755642e-01**
tanh stress RTiCM	3	-77.074089	1.567410	3.483934	1.035478e-14
step stress RTiCM	4	-77.988635	2.408014	4.398480	5.518179e-15
constant	5	-78.551989	0.899912	4.961834	0.000000e+00

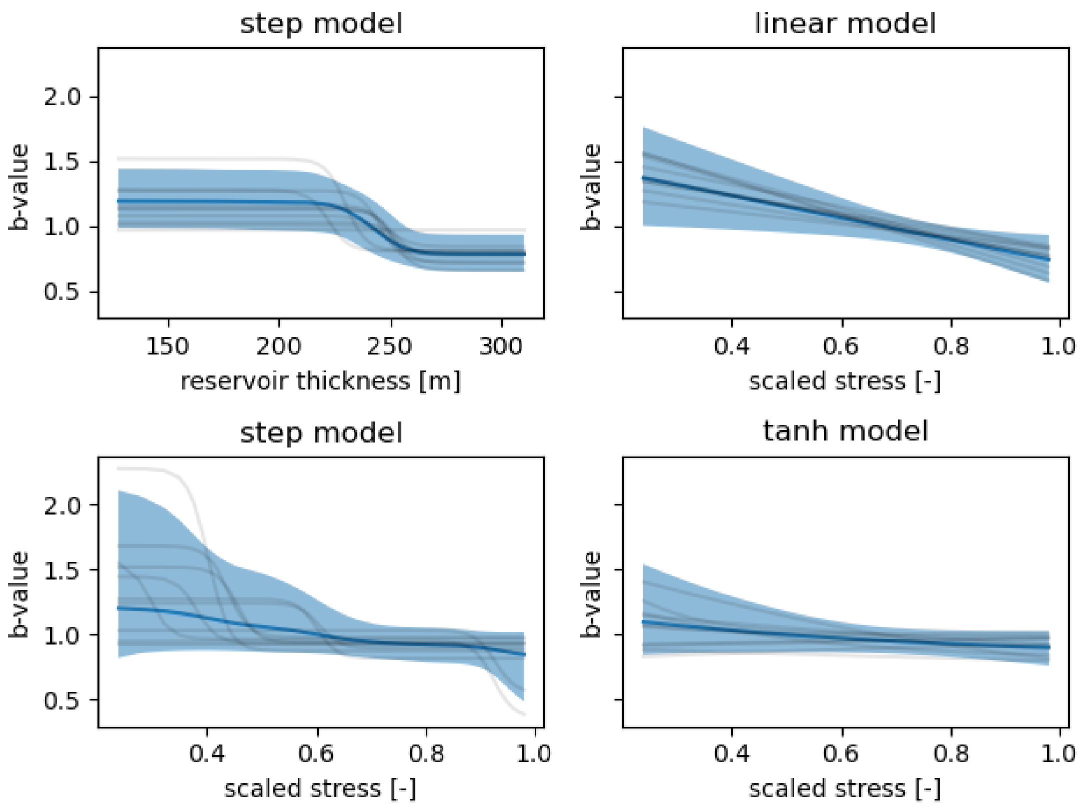

Figure 2.7: Posterior distributions of b-value as a function of reservoir thickness (m), top left, and as a function of scaled stress on the other graphs. The blue curves represent the expectation values, the blue bands represent the 95% confidence regions, while the grey lines represent random samples from the posterior model parameter distributions.

2.3.3 Wierden analysis

Dwelling mounds ('wierden' in Dutch) are anthropogenic structures constructed several centuries ago as a defence against flooding. As part of the development of the Ground Motion Model V7 (Bommer et al., 2022), Kruiver et al. (2022) characterized the dwelling mounds and developed a scheme to incorporate it into the seismic hazard and risk calculations. A final advice of SodM regarding the quality and suitability for usage of GMM-V7 in the pSHRA Groningen is still expected in 2023. Pending the full adoption of GMM-V7 in the pSHRA Groningen, an analysis was carried out to explore if the Wierden sub-model is suited for usage within GMM-V6.

For GMM-V7, Kruiver et al. (2022) derived a single penalty factor for all dwelling mounds in the public SHRA domain, which is only conditioned on the response period to address expected local amplification of ground motions. This penalty factor is based on a modeling study of the GMM-V7 site response model. This means that the amplification factor is strictly speaking only applicable for GMM-V7. It is expected that the use of the penalty factor in combination with GMM-V6 will lead to underestimation or overestimation of the ground motions and thus also the risk of buildings on mounds.

In general the application of the wierden sub-model results in a higher risk for the buildings situated on dwelling mounds. The most fragile buildings on wierden (LPR between 10^{-5} and 10^{-6}) show a 2.5 to 3 times higher risk after application of the wierden sub-model.

The risk results with application of the wierden sub-model were computed with both GMM-V6 and GMM-V7 models. The results based on GMM-V7 show a smaller relative increase in risk compared to GMM-V6. Applying the wierden penalty factor in combination with GMM-V6 appears to result in a higher risk assessment than would be expected on basis of GMM-V7. On average, the application of the GMM-V7-based penalty factor as an adjustment in GMM-V6 leads to an approximately 2 to 3% higher risk assessment (LPR) of buildings on dwelling mounds than the original GMM-V7 application.

Further validation of the penalty factor based on GMM-V6 is required before definitive conclusions can be drawn from this analysis. This is also a precondition before considering adopting this amendment in a future pSHRA Groningen.

2.3.4 Dynamic reservoir model

The spatiotemporal prediction of the pore pressure within the Groningen reservoir is an input parameter for the seismic hazard and risk analysis. The Groningen dynamic reservoir model was recently recalibrated by NAM (2023b) by incorporating the new data that has become available since the previous model update in 2018. The newly achieved history-match including some other model updates results in improvements of local mismatches, most noticeably in the Borgsweer area.

In addition to the Dynamic model update, the model was converted from the proprietary Shell MoReS/Dynamo software package to the widely used Eclipse software package (Schlumberger) by NAM (2023c). The model is available through the epos-nl.nl data portal. Eclipse models can potentially be converted to use within OPM Flow, an open source reservoir simulator (OPM | The Open Porous Media Initiative (opm-project.org). This facilitates further share and use of the reservoir model for research and educational activities.
TNO is currently testing and reviewing the to Eclipse format converted Groningen dynamic model.

2.3.5 NAM updated SSM calibration

Parallel to the TNO efforts on recalibrating the SSM for use in the yearly pSHRA Groningen, NAM (2023a) performed an update of their 2021 calibration using newly available earthquake data till January 2023.
The new calibration was evaluated by TNO. Overall the recalibrated model parameters showed improved statistical model performance compared to the previous NAM calibration of 2021. The 2023 NAM recalibration still underpredicts the total number of observed events significantly with 32 events.

3 Technical status TNO Model Chain Groningen

3.1 Updated model components

3.1.1 TNO-2023 Seismological Source Model

In this section we summarize the components of the *TNO-2023* SSM (Table 3.1). This model is largely based on the TNO-2020 SSM (TNO, 2020b) used for the pSHRA Groningen 2023.

Table 3.1: Overview of SSM version TNO-2023

SSM	documentation	TNO software implementation	HRA		pSHRA		
version			2019	2020	2021	2022	2023
TNO-2023	Bourne et al., 2019; TNO, 2022a; this report	TNO, 2020b					
Sub models							
TNO-Model calibration		TNO, 2020a					x
Coulomb stress distribution predictor for activity rate		TNO, 2020a					x
Activity rate		TNO, 2020a	x	x	x	x	x
Activity rate RTiCM		TNO, 2023b					
ETAS		TNO, 2020a	x	x	x	x	x
MD: linear stress dependent b-value & Mmax distribution		Kraaijpoel et al, 2022					
MD: step thickness dependent b-value & Mmax distribution		Kraaijpoel et al, 2022					

With respect to the current SSM the changes are limited to the following points:
- Implementation enhancements as described in paragraph 2.2.
- Introduction of the Rate-type compaction based activity rate model as described in paragraph 2.1.1 as an alternative to the current linear compaction based activity rate model.
- Replacement of the current hyperbolic tangent stress dependent b-value model with two alternative models: a linear stress dependent b-value model and a step thickness dependent b-value model, as described in Kraaijpoel et al, 2022.

In paragraph 2.3 a model weighting procedure is described. This procedure is not part of the model set used for the pSHRA Groningen, but a workflow to independently compare alternative models. The result of this workflow is used as a guidance to assign logic tree weights to both proposed activity rate and magnitude distribution models:
- A 50%-50% logic tree weighting of linear compaction and RTiCM based activity rate models, as described in paragraph 2.3.2.1.
- A logic tree weight distribution of the newly introduced b-value models: 70% step thickness and 30% linear stress, as described in paragraph 2.3.2.2.

3.2 Available model components

Apart from the above described newly introduced TNO-2023 SSM, the set of available model components is unchanged and described in the Model Chain status report 2022 (TNO, 2022a). Table 3.2 shows an overview of all available model components and indicates the usage in past HRA and/or pSHRA runs.
For future use TNO proposes to use the newly introduced TNO-2023 SSM, GMM-V7 and the TNO-2020 FCM. The latter two are unchanged and also proposed by TNO in 2022. The proposed associated logic tree is visualized in Figure 3.1.

Table 3.2: Overview of available model components and versions and TNO proposed model versions for future use.

model version	documentation	TNO software implementation	HRA		pSHRA			TNO proposal
			2019	2020	2021	2022	2023	
SSM								
NAM-V6	Bourne et al., 2019	TNO, 2020b		x	x	x		
TNO-2020	Bourne et al., 2019; TNO, 2022a	TNO, 2020b					x	
TNO-2023	Bourne et al., 2019; TNO, 2022a; this report	TNO, 2023b						x
SSM sub models								
TNO-Model calibration		TNO, 2020a					x	x
NAM-Model calibration provided as input		not part of HRA	x	x	x	x		
Single Coulomb stress conditioned to activity rate		TNO, 2020a	x					
Coulomb stress predictor for activity rate Coulomb stress predictor for magnitude distribution		TNO, 2020b		x	x	x		
Coulomb stress distribution predictor for activity rate		TNO, 2020a					x	x
Activity rate		TNO, 2020a	x	x	x	x	x	x
Activity rate RTiCM		TNO, 2023b						x
ETAS		TNO, 2020a	x	x	x	x	x	x
MD: constant b-value & Mmax distribution		TNO, 2020a						
MD: inverse power law b-value & Mmax distribution		TNO, 2020a	x					
MD: hyperbolic tangent b-value & Mmax distribution		TNO, 2020b		x	x	x	x	
MD: single b-value & exponential taper & Mmax distribution		TNO, 2020b		x	x	x		
MD: linear stress b-value & Mmax distribution		Kraaijpoel et al., 2022						x
MD: step thickness b-value & Mmax distribution		Kraaijpoel et al., 2022						x
GMM								
NAM-V7	Bommer et al., 2022	TNO, 2022b						x
NAM-V6	Bommer et al., 2019	TNO, 2020b		x			x	
NAM-V6-2021	Bommer et al., 2019	TNO, 2020b			x	x		
FCM								
TNO-2020	TNO, 2022a	TNO, 2020a						x
NAM-V7	Crowley and Pinho, 2020	TNO, 2020a		x	x	x	x	

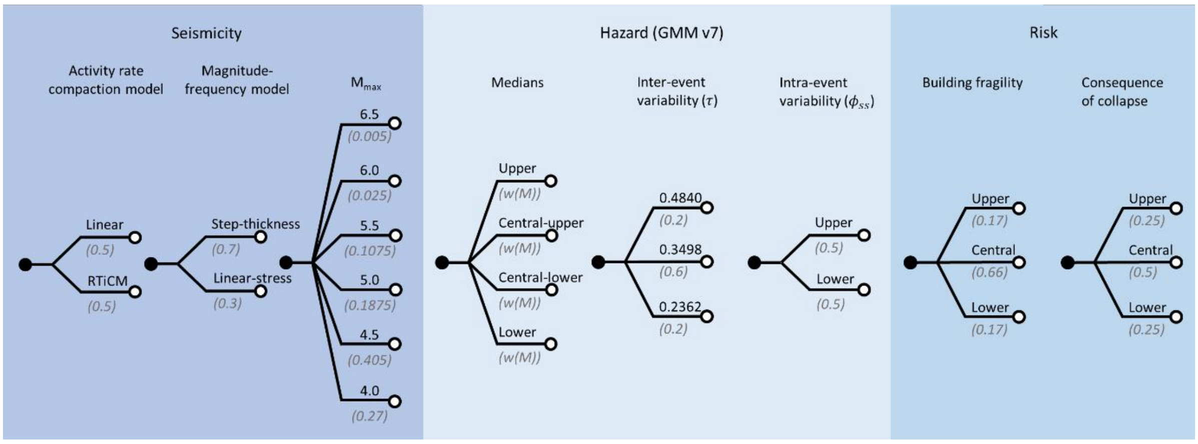

Figure 3.1: Logic tree structure, values and weights of the TNO proposed models for future pSHRA Groningen model runs. The TNO-2023 SSM introduces 2 new logic tree branches for both the activity rate compaction model (Linear and RTiCM) and the magnitude-frequency model (step-thickness and linear-stress).

References

Abril-Pla O, Andreani V, Carroll C, Dong L, Fonnesbeck CJ, Kochurov M, Kumar R, Lao J, Luhmann CC, Martin OA, Osthege M, Vieira R, Wiecki T, Zinkov R. (2023). PyMC: a modern, and comprehensive probabilistic programming framework in Python. *PeerJ Computer Science* 9:e1516, https://doi.org/10.7717/peerj-cs.1516.

Bommer, J., B. Edwards, P. Kruiver, A. Rodriguez-Marek, P. Stafford, B. Dost, M. Ntinalexis, E. Ruigrok and J. Spetzler (2019). V6 Ground-Motion Model (GMM) for Induced Seismicity in the Groningen Field With Assurance Letter, December 2019.

Bommer, J., Edwards B., Kruiver, P., Rodriguez-Marek, A., Stafford, P., Dost, B., Ntinalexis, M., Ruigrok, E. and Jesper Spetzler, J., (2022). V7 Ground-Motion Model for Induced Seismicity in the Groningen Gas Field (Update) With Assurance Letter. NAM Report.

Bourne, S. J., & Oates, S. J. (2017). Extreme threshold failures within a heterogeneous elastic thin sheet and the spatial-temporal development of induced seismicity within the Groningen gas field. Journal of Geophysical Research: Solid Earth, 122, 10,299–10,320, https://doi.org/10.1002/2017JB014356.

Bourne, S. J. & Oates, S. J. (2019). Evolution of induced earthquake magnitude distributions with increasing stress in the Groningen gas field, Restricted Draft, NAM, November 2019.

Crowley, H. & Pinho, R. (2020). Report on the Fragility and Consequence Models for the Groningen Field (version 7), March 2020.

Dieterich J. (1994). A constitutive law for rate of earthquake production and its application to earthquake clustering, J. geophys. Res.: Solid Earth, 99(B2), 2601–2618.

Gelman, Andrew, Jessica Hwang and Aki Vehtari (2014). Understanding predictive information criteria for Bayesian models. Stat Comput 24:997-1016, doi:10.1007/s11222-013-9416-2.

Heimisson, E.R., Smith, J.D., Avouac, J.-P., Bourne, S.J. (2022). Coulomb threshold rate-and-state model for fault reactivation: application to induced seismicity at Groningen, Geophysical Journal International, 228, 2061–2072.

Kraaijpoel, D., Martins, J., Osinga, S., Vogelaar, B., & Breunese, J. (2022). Statistical analysis of static and dynamic predictors for seismic b-value variations in the Groningen gas field. Netherlands Journal of Geosciences, 101, E18, doi:10.1017/njg.2022.15.

Kruiver, P., Pefkos, M., Meijles, E., Aalbersberg, G., Campman, X., van der Veen, W., Martin, A., Ooms-Asshoff, K., Bommer, J., Rodriguez-Marek, A. (2022). Incorporating dwelling mounds into induced seismic risk analysis for the Groningen gas field in the Netherlands, Bulletin of Earthquake Engineering (2022), 20:255-285.

Kumar et al., (2019). ArviZ a unified library for exploratory analysis of Bayesian models in Python. Journal of Open Source Software, 4(33), 1143, https://doi.org/10.21105/joss.01143.

NAM (2021). Groningen long term subsidence forecast, reference EP202008201822.

NAM (2023a). Recalibration of the Seismicity Model, 3 February 2023.

NAM (2023b). Groningen Dynamic Model Update 2023, June 2023, reference EP202306200914.

NAM (2023c). Dynamic Model (Eclipse Version) to predict the formation pressure response to gas extraction in the Groningen gas field, The Netherlands, 7 September 2023, https://doi.org/10.24416/UU01-8JYW40.

Pruiksma, J. P., Breunese, J. N., van Thienen-Visser, K., & De Waal, J. A. (2015). Isotach formulation of the rate type compaction model for sandstone. International Journal of Rock Mechanics and Mining Sciences, 78, 127-132.

TNO (2019). Comparative analysis of the NAM and TNO implementation in the Groningen Seismic Hazard and Risk Assessment, TNO 2019 R11997.

TNO (2020a). Probabilistic Seismic Hazard and Risk Analysis in the TNO Model Chain Groningen. TNO 2020 R11052.

TNO (2020b). TNO Model Chain Groningen: Update and quick scan comparison of 2020 HRA model, TNO 2020 R11659, 6 November 2020.

TNO (2022a). Status of the TNO Model Chain Groningen per October 1, 2022 and recommendations for the public Seismic Hazard and Risk Analysis 2023, TNO 2022 R11961, 18 oktober 2022.

TNO (2022b). Implementation of GMM-V7 in the TNO Model Chain, TNO 2022 R10801, final draft, 18 July 2022.

TNO (2022c). KEM9: Cumulative propagation effect of Groningen risk model component uncertainties on hazard and risk predictions, TNO 2021 R12442, 9 September 2022.

TNO (2023a). Wierdenanalyse in GMM-V6: Risicoanalyse van gebouwen op wierden met en zonder toepassing van een aangepast opslingermodel in Grondbewegingsmodel V6, Memo AGE 23-10.059, 19 juni 2023.

TNO (2023b). Implementation and model performance of Rate-type compaction based Seismological Source Model, TNO 2023 R11796, 4 October 2023.

Rhoades, David A., Danijel Schorlemmer, Matthew C. Gerstenberger, Annemarie Christophersen, J. Douglas Zechar, Masajiro Imoto (2011). Efficient testing of earthquake forecasting models. Acta Geophysica, 59:728-744, doi:10.2478/s11600-011-0013-5.

Savran, William H., José A. Bayona, Pablo Iturrieta, Khawaja M. Asim, Han Bao, Kirsty Bayliss, Marcus Herrmann, Danijel Schorlemmer, Philip J. Maechling, Maximilian J. Werner (2022). pyCSEP: A Python Toolkit for Earthquake Forecast Developers. Seismological Research Letters 2022; 93 (5): 2858–2870, doi: https://doi.org/10.1785/0220220033.

Smith J.D., Heimisson E.R., Bourne S.J., Avouac J.-P., (2022). Stress-based forecasting of induced seismicity with instantaneous earthquake failure functions: applications to the groningen gas reservoir. Earth and Planetary Science Letters, 594, 117697.

Vehtari, Aki, Andrew Gelman and Jonah Gabry (2017). Practical Bayesian model evaluation using leave-one-out cross-validation and WAIC. Stat Comput (2017) 27:1413-1432, doi:10.1007/s11222-016-9696-4.

de Waal, J. A. (1986). On the rate type compaction behaviour of sandstone reservoir rock. Doctoral dissertation, Technische Universiteit Delft.

Yao, Yuling, Aki Vehtari, Daniel Simpson, and Andrew Gelman (2018). Using stacking to average bayesian predictive distributions (with discussion). Bayesian Analysis, sep 2018, doi:10.1214/17-ba1091.

Signature

TNO › Energy & Materials Transition › Utrecht, 11 October 2023

R. van Steveninck
Research manager

M.P.D. Pluymaekers
Author

Energy & Materials Transition

Princetonlaan 6
3584 CB Utrecht
www.tno.nl